ASIAN JOURNAL OF CIVIL ENGINEERING (BUILDING AND HOUSING) VOL. 6, NO. 4 (2005)
PAGES 303-315

EFFECT OF SHELL GEOMETRY AND MATERIAL CONSTANTS ON DYNAMIC BUCKLING LOAD OF ELASTIC PERFECT CLAMPED SPHERICAL CAPS

S. Taeprasartsit[*a], K. Tao[b]
[a]Department of Mechanical Engineering, Toyohashi University of Technology, Tempaku-cho Toyohashi 441-8580, Japan
[b]Department of Mechanical Engineering, Suzuka National College of Technology, Shiroko-cho Suzuka 510-0294, Japan

ABSTRACT

A numerical experiment using the finite element method to show that the nondimensional dynamic buckling pressure of deep elastic isotropic clamped perfect spherical caps subjected to suddenly applied uniform pressure is represented by a function of the geometric parameter and the thickness to radius ratio of caps. Three definitions of geometric parameter are considered. The effects of material properties are also taken to consideration.

Keywords: structural analysis; dynamic buckling; spherical caps; axisymmetric snap-through; finite element method

1. INTRODUCTION

The analysis of axisymmetric dynamic snap-through of elastic clamped shallow spherical shells has been reported in a large number of research papers. The most important pioneers in this branch of study are Budiansky and Roth [1] who proposed a criterion to predict the dynamic buckling pressure of shallow spherical shells. Later then, the study in this topic has received considerable attention. Important papers are Simitses [2], Huang [3], Stephens and Fulton [4], Ball and Burt [5], and Stricklin and Martinez [6]. Also, experiments have been performed and reported by Lock et al. [7] and Humphreys et al. [8]. Reviews on the subject have been given by Ball [9] and Holzer [10].

To the authors' knowledge, most of the researches in this topic for the case of isotropic shells are based on thin shell theory together with shallow shell assumptions. So the applicable range of the existing solution is limited by the assumptions used in shallow thin shell theory. In those research papers, the nondimensional dynamic buckling pressure, p_{cr} is considered to be a function of the geometric parameter, λ only. However, a question arises here that if we use the finite element method, do two caps having the same value of λ but

[*] Email-address of the corresponding author: tsompon@hotmail.com

very different geometrical aspects still have the same value of p_{cr}? There are three objectives in the present study. First, to approve the suitability of considering that p_{cr} is a function of λ only. Second, to study the effect of using different definitions of λ. Three definitions of λ are taken to consideration. Third, to study the effect of material properties on p_{cr}. These works are done by doing a large number of numerical examples using the finite element method. Because the caps in our study have a wide range of geometrical aspects ranging from thin to thick and from shallow to deep, then thin shell finite element is not adopted in this study. Instead, we use 4-noded quadrilateral axisymmetric finite element based on large-deformation elasticity theory.

To avoid programming errors, the authors choose to not invent our own finite element program. The world-wide used and highly reliable finite element software ANSYS is used throughout this study.

2. COMPUTATIONAL PROCEDURE

2.1 Problem description

A clamped spherical cap with central height *H*, base radius *a*, semi-angle *α*, and uniform thickness *h*, under a suddenly applied uniform pressure *q* acting on its top surface as shown in Figure. 1 is taken to consider. Many research papers (e.g. [1], [3]) have used two approximations related to the geometry of caps. One is that the undeformed shape of the cap is described by parabolic relationship

$$z_0 = H\left[1 - \left(r^2 / a^2\right)\right] \tag{1}$$

where *r* is the radial coordinate. The other approximation is that the radius of the cap is expressed approximately as

$$R = a^2 / 2H \tag{2}$$

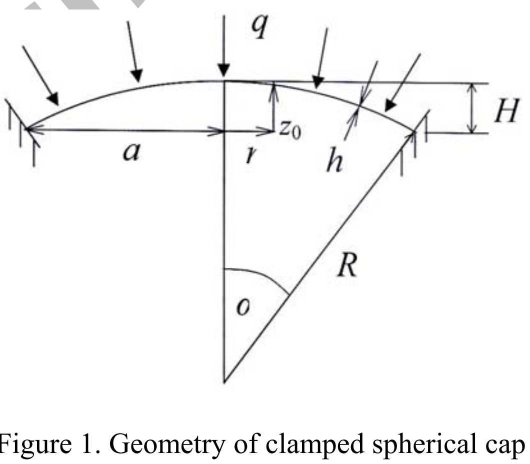

Figure 1. Geometry of clamped spherical cap

However, in this study we do not use these approximations. Our geometrical model is exactly circular arc, not parabola, so R is expressed by

$$R = \left(a^2 + H^2\right)/2H \tag{3}$$

The following dimensionless parameters are used.

1. geometric parameter; In the present study three definitions of λ are taken to consideration. All of them were originally proposed in the study of static buckling of spherical caps. The first definition of λ is defined without using shallowness assumptions and here we name it λ_1,

$$\lambda_1 = \sqrt[4]{12\left(1-\nu^2\right)}\sqrt{R/h}\,\alpha \tag{4}$$

where ν is Poisson's ratio. The second definition of λ is named λ_2 and it is derived from Eq. (4) by using a shallowness assumption α<<1 that made $R\alpha$ E a, then

$$\lambda_2 = \sqrt[4]{12\left(1-\nu^2\right)}\left(a/\sqrt{Rh}\right) \tag{5}$$

And the third one named λ_3 is from Eq. (5) with the assumption of Eq. (2), then

$$\lambda_3 = 2\sqrt[4]{3\left(1-\nu^2\right)}\left(H/h\right)^{1/2} \tag{6}$$

To the authors' knowledge, all research papers in the topic of dynamic buckling of spherical caps use only λ_3 as the geometric parameter. λ_2 is used in some papers in the topic of static buckling, e.g. [11].

2. nondimensional pressure;

$$p = q/q_0 \tag{7}$$

where q_0 is the classical static buckling pressure of a complete spherical shell of the same radius of curvature and thickness.

$$q_0 = \frac{2E}{\sqrt{3\left(1-\nu^2\right)}}\left(\frac{h}{R}\right)^2 \tag{8}$$

where E is Young's modulus.

3. nondimensional time;

$$\tau = \frac{t}{R}\sqrt{\frac{E}{\rho}} \tag{9}$$

where t is time and ρ is mass per unit volume.

2.2 Numerical methods

To avoid any errors that might occur during the programming process, the authors decide to use ANSYS. The program contains many features to deal with geometric nonlinearity.

1. finite element : We use the 2D 4-noded quadrilateral elements (PLANE42). The element is used as an axisymmetric element.

2. transient dynamic analysis : The effect of damping is not included. Then the equation of motion of this analysis is

$$[M]\{\ddot{u}\}+[K]\{u\}=\{F\} \tag{10}$$

where $[M]$ and $[K]$ are system mass and stiffness matrices, $\{u\}$ and $\{F\}$ are the nodal displacement and nodal applied load vectors. The Newmark method is used for time integration.

3. geometric nonlinear analysis : We use the large strain analysis. The Newton-Raphson method is employed to solve nonlinear equations.

4. dynamic buckling criterion : Although criteria for dynamic buckling of spherical caps are not well defined, the criterion suggested by Budiansky and Roth [1] is the most widely used. The criterion is based on plots of the peak nondimensional average displacement, Δ_{max}, of the cap in time history versus the magnitude of the nondimensional load, p. This average displacement Δ has been defined as follows,

$$\Delta = \int_0^a rw\,dr \bigg/ \int_0^a r z_0\,dr \tag{11}$$

where $w(r,t)$ is vertical displacement. The load corresponding to a sudden jump in Δ_{max} is taken as the dynamic buckling load. Instead of Δ some of the studies use w at the apex (here we give + for w if it points upward and the minimum w is the largest minus w), and plots of minimum w at the apex versus the load predict the dynamic buckling load. In this study we decided to use w at the apex because after solving some problems we found that both criteria lead to the same buckling loads. The criterion of using w at the apex is demonstrated by a typical example shown in Figures. 2 and 3. Figure 2 represents the displacement at the apex w_{apex}-τ curves for different values of p for a clamped spherical cap of 0.5 mm thickness, 1 m radius and λ_3=5. A plot of the variation of minimum w_{apex} with respect to p associated with Figure. 2 is shown in Figure. 3. A sharp drop at p=0.436 is clear, and according to the dynamic buckling criterion described above, this value of p is taken as dynamic buckling pressure p_{cr} for this cap. Note that in the present study, the precision of p_{cr} is three significant digits while most of other papers consider only two digits.

3. NUMERICAL RESULTS AND DISCUSSION

First of all, let us set up the criteria to select the number of elements and the time step size. The length of calculation time τ is taken as 75 but time may be extended to allow $w_{apex} - \tau$ curves to fully develop.

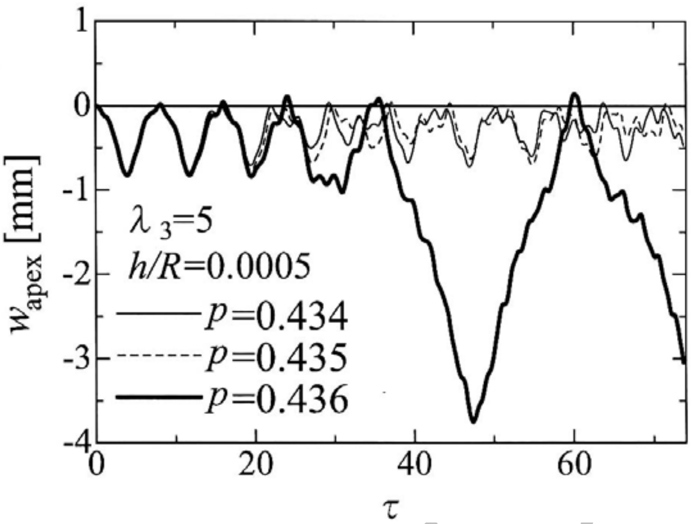

Figure 2. Variations of w at the apex with time (h=0.5 mm, R=1 m, λ_3=5)

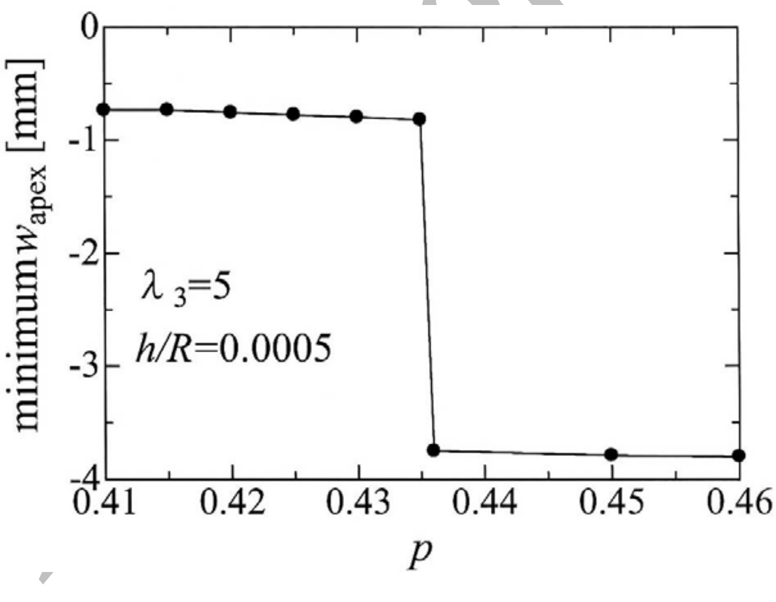

Figure 3. Decision of dynamic buckling load p_{cr} (h=0.5 mm, R=1 m, λ_3=5)

1. time step size: We choose the time step size Δτ=0.075 for the Newmark time integration scheme. However, in the case that caps are very thick that cause divergent in equation solving process, we rather use the automatic time stepping ability built in ANSYS.

2. number of elements: Because we have to solve a large number of problems of a wide range of geometrical sizes, it is the best to use automatic meshing ability. In case of ANSYS this can be done by using the command SMRTSIZE,*n* where *n* is an integer value from 1 (fine mesh) to 10 (coarse mesh). In this study, in order to gain results with high accuracy, we use SMRTSIZE,1 throughout the study.

To verify the validity of the numerical method, we compare our results with others for the case of thin shallow caps. The results are shown in Table 1. Note that all results in Table 1 are for ν=0.3 or 1/3.

Table 1. Dynamic buckling pressure p_{cr} for various values of geometric parameter λ_3

λ_3	4	5	6	7.5	10
H/h (Eq. (6), ν=0.3)	2.42	3.78	5.45	8.51	15.13
Present (h/R=10^{-4}, ν=0.3)	0.439	0.437	0.580	0.440	0.355
Ganapathi et. al. [12]	0.455	0.460	0.605	0.450	0.495
Huang [3]	0.45	0.49	---	0.50	0.42
Stephens et. al. [4]	---	0.45	0.62	0.44	0.37

According to Table 1, although there are some differences among the literature, the present values are in reasonably good agreement with those ones.

From the results of caps of various depth and thickness, we found that caps of the same λ (λ_1 or λ_2 or λ_3) and h/R always have exactly the same value of p_{cr}. That means p_{cr} is a function of both λ and h/R. The choice of definition of λ does not change this conclusion. Because H/a is a function of λ and h/R, then we can also state that p_{cr} is a function of both λ and H/a. The expressions of H/a as a function of λ and h/R are as follows:

From Eq. (4),
$$\frac{H}{a}=\frac{1}{\tan\left(\frac{\pi}{2}-\frac{0.5\lambda_1}{\sqrt[4]{12\left(1-\nu^2\right)}}\sqrt{\frac{h}{R}}\right)} \tag{12}$$

From Eqs. (3) and (5),
$$\frac{H}{a}=D-\sqrt{D^2-1} \tag{13}$$

Where

$$D=\frac{\sqrt[4]{12\left(1-\nu^2\right)}}{\lambda_2}\sqrt{\frac{R}{h}} \tag{14}$$

From Eqs. (3) and (6),

$$\frac{\mathrm{H}}{\mathrm{a}} = \left(\frac{\lambda_3^{\ 2}}{(\mathrm{R}/\mathrm{h})\sqrt{192(1-\nu^2)} - \lambda_3^{\ 2}} \right)^{1/2} \tag{15}$$

Furthermore, using the fact that α is a function of *H/a*,

$$\alpha = 2\tan^{-1}(\mathrm{H}/\mathrm{a}) \tag{16}$$

we can also conclude that p_{cr} is a function of *h/R* and α.
The results for λ_3= 5 are shown in Table 2 and Figure. 4.

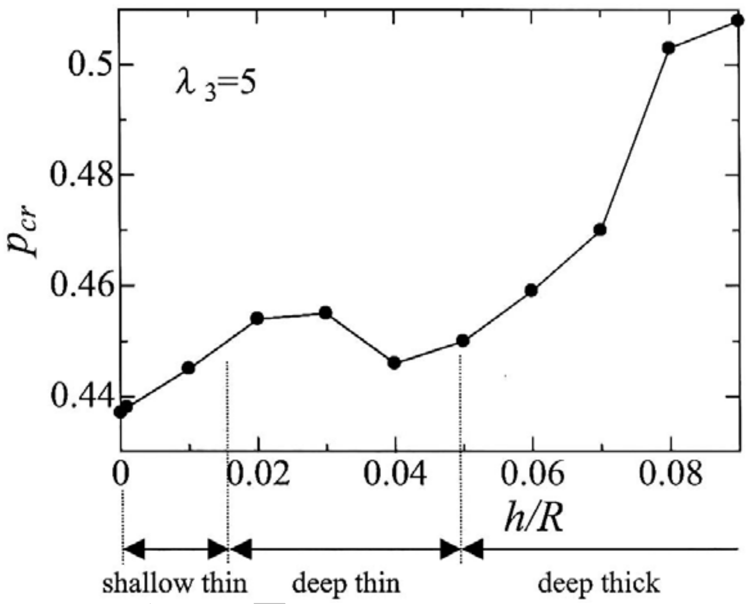

Figure 4. Variation of p_{cr} for λ□=5 with *h/R*

Table 2. Dynamic buckling pressure p_{cr} for λ_3=5 (ν=0.3)

h/R **(corresponding *H/a*)**	p_{cr}	***h/R*** **(corresponding *H/a*)**	p_{cr}
0.0001 (0.014)	0.437	0.05 (0.323)	0.450
0.001 (0.044)	0.438	0.06 (0.358)	0.459
0.01 (0.139)	0.445	0.07 (0.391)	0.470
0.02 (0.198)	0.454	0.08 (0.422)	0.503
0.03 (0.245)	0.455	0.09 (0.453)	0.508
0.04 (0.286)	0.446		

The definition of thin shells is $h/R < 0.05$ and according to Reissner [13], a spherical shell is called “shallow” if $H/a \leq 1/6$ (=0.167). Then the first three rows (of the first two columns) of Table 2 are for shallow thin caps, the next three rows are for deep thin caps, and the remaining rows are for deep thick caps.

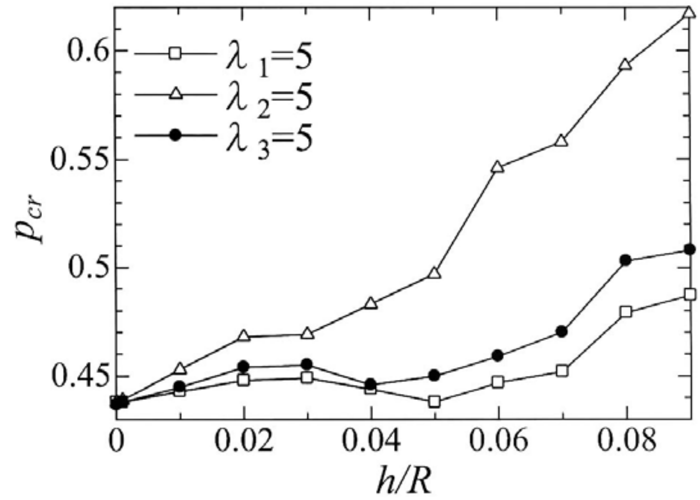

Figure 5. Variations of p_{cr} for $\lambda = 5$ with h/R

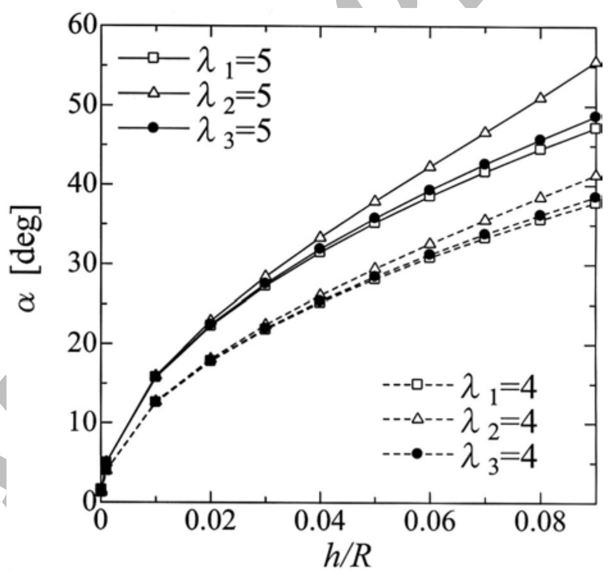

Figure 6. Variations of semi-angle α for $\lambda=4$ and 5 with h/R

Figure 5 shows the results for three definitions of $\lambda = 5$. The results for λ_2 case are evidently apart from the results for the other two cases. This can be explained by considering Figure. 6 as we can see the difference of depth between λ_2 case and the other two cases. And it should be noted that while λ_3 uses more approximation than λ_2, its corresponding geometry of caps is closer to the one for λ_1. As we can see from Figure. 5, for λ=5 the choice of λ is almost immaterial in the range of shallow caps, but it becomes significant when caps are very deep. In the case of shallow thin caps, the way that all papers in the past consider p_{cr} as a function of λ_3 only is undoubtedly suitable. However, if we need an exact value of p_{cr} for a specific geometry of caps, we should consider p_{cr} as a function of both λ and *h/R* (or *H/a*).

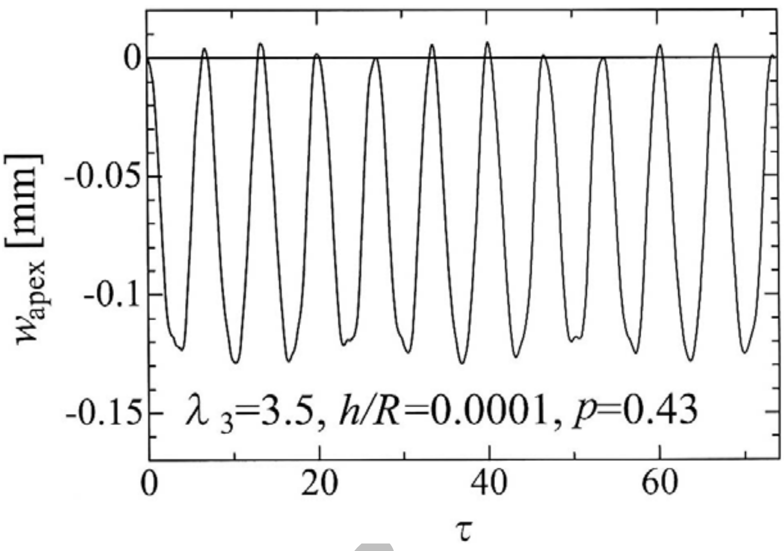

Figure 7. Dynamic response of λ_3=3.5 caps (h=0.1 mm, R=1 m) under p=0.43

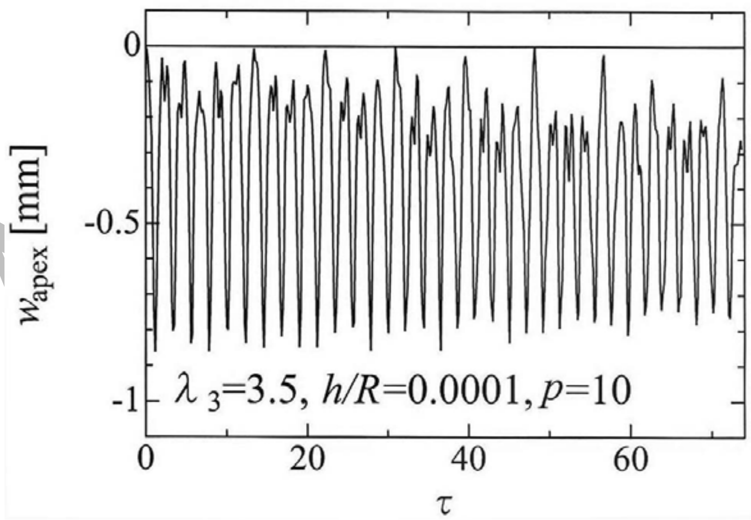

Figure 8. Dynamic response of λ_3=3.5 caps (h=0.1 mm, R=1 m) under p=10

Next, let us consider the case of $\lambda = 4$. As well known, for small values of λ, say $\lambda<4$, the vibrating behavior of caps is close to circular plate. Figures 7 and 8 show the w_{apex}-τ graphs for λ_3=3.5 under moderate and very large pressure, respectively. From those figures, we can conclude that the sudden drop of the minimum w_{apex} does not occur for those caps of small values of λ. Under very large pressure, caps only vibrate at higher amplitude and frequency. In case of $\lambda_3 = 4$ caps, see Figures. 9 and 10, we find that their behavior is between the two in Figures. 2 and 7. That is although the sharp drop of the minimum w_{apex} in a time interval still occurs, it is quite not clear, especially in Figure. 10. This causes difficulty in using the Budiansky-Roth criterion. This behavior occurs for all λ_1, λ_2 and λ_3=4 caps, no matter *h/R* is. Figure 11 shows the results of p_{cr} for three definitions of $\lambda = 4$. Again, the results for λ_2 case are apart from the results for the other two cases.

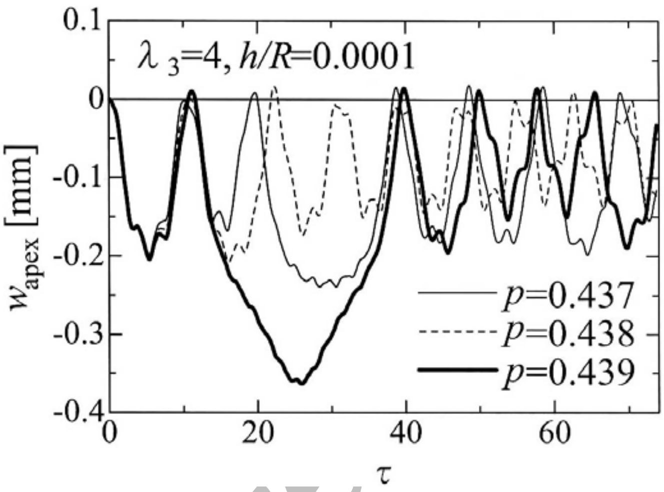

Figure 9. Dynamic response of λ_3=4 caps (h=0.1 mm, R=1 m)

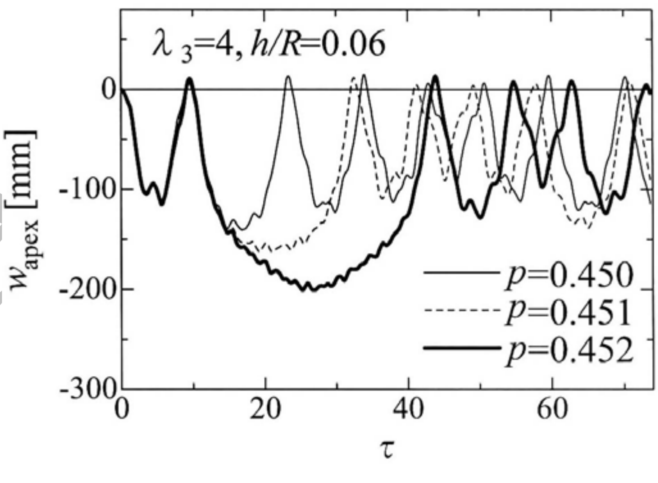

Figure 10. Dynamic response of λ_3=4 caps (h=60 mm, R=1 m)

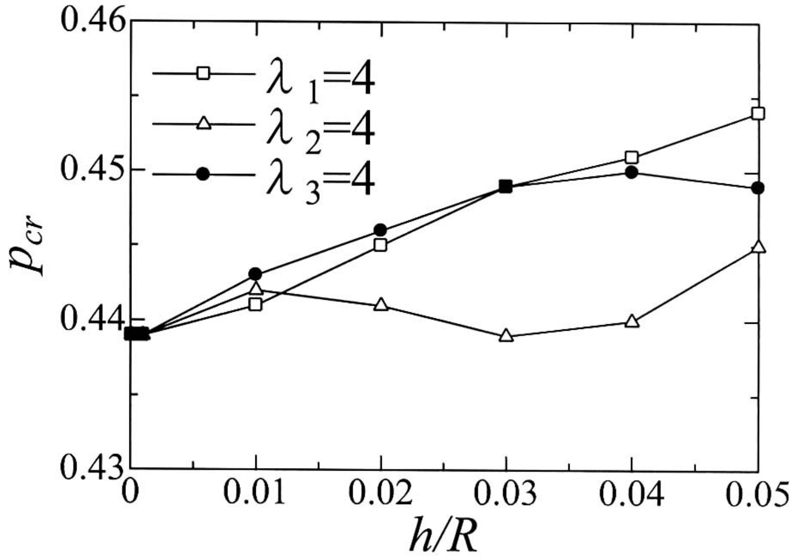

Figure 11. Variations of p_{cr} for $\lambda = 4$ with h/R

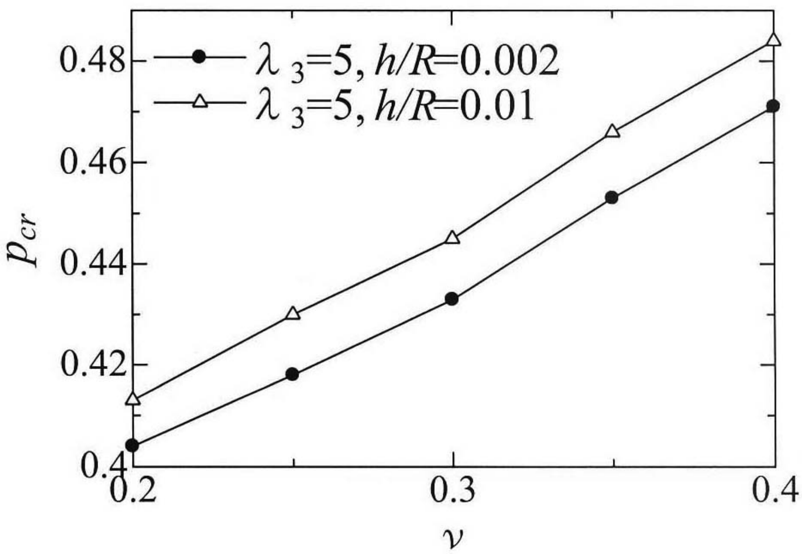

Figure 12. Variations of p_{cr} with respect to v

Finally, we do some calculation to investigate the effect of material properties on p_{cr}. The material properties related in this study are E, ρ and v. We found that E and ρ do not affect p_{cr} whereas v greatly affects p_{cr}. Note that all results presented above are for E=193 GPa, ρ=8000 kg/m^3, v=0.3. The relation between p_{cr} and v is nearly linear in the range $0.2 \le v \le 0.4$ as shown in Figure. 12 for two examples of geometry of caps.

4. CONCLUSIONS

By using the finite element method based on large-deformation elasticity theory to study the behavior of axisymmetric dynamic buckling of elastic clamped spherical caps, the following conclusions can be drawn:

1. No matter which definition of geometric parameter λ in Eqs. (4)-(6) we use, the nondimensional dynamic buckling pressure p_{cr} is truly a function of λ and the thickness to radius ratio h/R (or the central height to base radius ratio H/a). To avoid using λ, we can also state that p_{cr} is a function of h/R and semi-angle α.

2. At given values of λ and h/R, using different definitions of λ gives us caps of different depth. Although λ_3 uses more approximation than λ_2, its corresponding geometry of caps is closer to the geometry of caps of λ_1. Consequently, p_{cr} for λ_1 and λ_3 are close to each other, while p_{cr} for λ_2 is quite apart from those of the other two λ's.

3. For λ=4, the sharp drop of the minimum w_{apex} in a time interval is relatively not clear comparing with λ=5 case. And the clarity of sharp drop depends primarily on λ only.

4. Among the material properties Young's modulus E, density ρ and Poisson's ratio v, we find that v is the only one that affect p_{cr} and the relation between p_{cr} and v is nearly linear in the range $0.2 \leq v \leq 0.4$.

REFERENCES

1. Budiansky, B. and Roth, R.S. Axisymmetric dynamic buckling of clamped shallow spherical shells. *NASA* TN D-1510, (1962)597-606.
2. Simitses, G.J. Axisymmetric dynamic snap-through buckling of shallow spherical caps. *A.I.A.A. J.* **5** (5), (1967)1019-1021.
3. Huang, N.C. Axisymmetric dynamic snap-through of elastic clamped shallow spherical shells. *A.I.A.A. J.* **7** (2), (1969)215-220.
4. Stephens, W.B. and Fulton, R.E. Axisymmetric static and dynamic buckling of spherical caps due to centrally distributed pressure. *A.I.A.A. J.,* **7** (11), (1969)2120-2126.
5. Ball, R. E. and Burt, J. A., Dynamic buckling of shallow spherical shells. *J. Appl. Mech.* **40**, (1973)411-416.
6. Stricklin, J. A. and Martinez, J.E. Dynamic buckling of clamped spherical caps under step pressure loadings. *A.I.A.A. J.* **7** (6), (1969)1212-1213.
7. Lock, M.H. Okubo, S. and Whittier, J.S. Experiments on the snapping of a shallow dome under a step pressure load. *A.I.A.A. J.,* **6** (7), (1968)1320-1326.
8. Humphreys, J.S. Roth, R.S. and Zatlers, J., Experiments on dynamic buckling of shallow spherical shells under shock loading. *A.I.A.A. J.,* **3** (1), (1965)33-39.
9. Ball, R.E. Dynamic buckling of structures. *Shock and Vibration Computer Programs: Reviews and Summaries* (edited by W. Pilkey and B. Pilkey), Shock and Vibration Information Center, Washington, D.C., (1975)299-321.
10. Holzer, S.M. Dynamic snap-through of shallow arches and spherical caps. *Shock Vibration Digest,* **11** (3), (1979)3-6.

11. Uchiyama, M. and Yamada, S. Nonlinear buckling simulations of imperfect shell domes by mixed finite elements. *ASCE J. of Engineering Mechanics,* **129**(7), (2003)707-714.
12. Ganapathi, M. and Varadan, T.K. Dynamic buckling of laminated anisotropic spherical caps. *ASME Journal of Applied Mechanics,* **62**(1995)13-19.
13. Reissner, E. Symmetric bending of shallow shells of revolutions. *Journal of Mathematics and Mechanics,* **7**(1958) p.121.